



February 4, 2015

ESI Project: 47357A

# 3-D Printer Nozzle Failure Analysis

## Report Prepared for:

Mr. Brent MacKenzie  
Aleph Objects, Inc.  
626 West 66th Street  
Loveland, CO 80538

## Summary and Conclusions

---

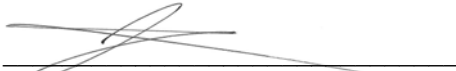
1. The subject nozzles meet the chemical requirements of ASTM B 194-08 for a C17200 beryllium copper.
2. The subject nozzles identified as A and B, which failed in service, suffered intergranular cracking.
3. Failure of the subject nozzles was delayed, occurring after a period of time in service, and at elevated temperatures (210 – 300 °C).
4. There was no evidence of branch cracking indicative of stress corrosion cracking (SCC).
5. The most likely cause of failure was hydrogen embrittlement of oxygen-rich copper alloy.
  - a. Hydrogen-oxygen embrittlement occurs when hydrogen diffusing into the copper reacts with oxygen in the copper forming water vapor at the copper grain boundaries.
  - b. The water vapor imparts a stress at the grain boundaries, causing grain boundary decohesion and embrittlement.
  - c. The presence of dimpled-rupture at the grain boundaries, the lack of observable grain boundary precipitates, and the time interval in service before failure indicates hydrogen-oxygen embrittlement as the cause of failure.
6. Preventative actions against future failure include:
  - a. Add a radius of curvature to the nozzle threaded section/head junction to reduce the stress intensity at this location.
  - b. Require a materials specification for a low oxygen containing copper alloy.
  - c. Specify that the nozzle heat treatment be performed in a hydrogen free environment.
  - d. Require a materials specification for a non-copper based alloy such as stainless steel.

This report and its contents are the Work Product of Engineering Systems Inc. (ESI). This report should only be duplicated or distributed in its entirety. This report may contain confidential or court protected information; please contact an authorized entity prior to distributing. Conclusions reached and opinions offered in this report are based upon the data and information available to ESI at the time of this report, and may be subject to revision after the date of publication, as additional information or data becomes available.

Copyright ESI © 2015 - All Rights Reserved

Phone: 630-851-4566 ■ Fax: 630-851-4870 ■ Toll Free: 866-596-3994

**Reviewed by:**



Jacob D. Fuerst, Ph.D  
Staff Consultant

**Reviewed by:**



Ronald J. Parrington, P.E., FASM  
Director of Industrial Services &  
Senior Managing Consultant

---

## Introduction and Background

---

Engineering Systems, Inc., (ESI) was contracted by Aleph Objects, Inc., to perform an evaluation and failure analysis of several subject copper alloy nozzles used as the extrusion tips in a polymeric 3-D printer. The provided brass nozzles were identified as groups A, B, C, D, E, F, and G. Nozzles A and B failed while in service. Nozzles C and D were used in service but did not fail. Nozzles E and F failed by being subjected to overstress by Aleph Objects, Inc., to attempt to reproduce the in-service failures of nozzles A and B. Nozzle group G was a selection of unused exemplar nozzles for evaluation. In addition, a nozzle from an alternate source was submitted for chemical analysis.

---

## Testing

---

### Optical Microscopy and SEM

The subject nozzles were photographed in the as received condition (Figures 1-7). The threaded section of the nozzles had fractured away from the nozzle heads at the threaded section/head junction. A review of provided design drawings for the nozzle show that the junction angle between the threaded section and head appears to be a corner with no specified radius of curvature, indicating a significant stress riser at this location (Figure 8). The design drawings provided no materials specification for the manufacture of the nozzles.

Subject nozzles A, B, and F were then examined using stereo-optical microscopy. The fracture surfaces of nozzles A and B appeared to be intergranular (Figures 9-10). The fracture surface of nozzle F, which had been over torqued until failure, appeared to be ductile failure (Figures 11). Scanning Electron Microscopy (SEM) was performed on nozzles A and B, confirming the intergranular fracture of the material (Figures 12-13).

Nozzles A, B, and F were then cleaned by ultra sonication in acetone to and reexamined with stereo-optical microscopy and SEM. Cleaning of the fractures surfaces allowed SEM to be performed at higher magnification and producing better resolution of the fracture surfaces. High magnification (500x and 1,000x) SEM imaging of the fracture surface of nozzle B showed texturing, appearing to be dimpled rupture, on the grain boundary surfaces (Figures 14-15). The fracture surface of nozzle F was revealed to be a mix mode fracture with regions showing typical dimpled rupture overload of a ductile material as well as regions of intergranular cracking (Figure 16). At this time Energy Dispersive x-ray Spectroscopy (EDS) was performed on the cleaned fracture surfaces of nozzles A and B, revealing peaks of primarily copper with additional peaks of oxygen and carbon, which was assumed to be residual polymeric material (Figures 17-18).

An exemplar nozzle from sample set G was then sectioned using a diamond impregnated cutting wheel, to remove the threaded section from the head of the nozzle. This threaded section was then placed in a bench-top vice and squeezed until failure occurred. There was little plastic deformation of the threaded section before cracking. The fracture surfaces of the broken exemplar nozzle were then examined using SEM. The fracture surface appeared to be mixed mode consisting of intergranular fracture and ductile overload (Figure 19). At high magnification (3,000x), the grain boundary surfaces appeared to show dimpled rupture (Figure 20).

### Metallography

The heads of nozzles A, B, and F, as well as the threaded section of nozzle A, and an exemplar from group G, were sectioned laterally using a diamond impregnated cutting wheel. The cross sections of the nozzles were then

mounted in Buehler EpoMet, thermoset epoxy, and polished using successively 240, 400, 600 grit SiC, 9µm diamond suspension, and 0.05µm alumina suspension.

Metallography of the cross sections of the fracture surfaces of samples A and B showed no branch cracking, which would be associated with stress corrosion cracking (SCC) (Figures 21-23). There were some small cracks observed at the grain boundaries in the bulk material (Figure 24). No grain boundary precipitates were observed.

The polished cross section of the threaded section of nozzle A was then evaluated using SEM. The grain boundary cracks were interrupted, appearing to be a series of interconnected voids (Figure 25).

## Chemistry Analysis

Nozzle C, which has been used in service but had not failed, and an exemplar nozzle from group G were sent to a qualified laboratory for chemical analysis (Table 1). The analysis of the nozzles was consistent with ASTM B 194-08 for a C17200 beryllium copper. Note, beryllium was not detected using EDS as it is below the molecular weight for elements that can be identified by the EDS detector used by ESI. Energy Dispersive x-ray Spectroscopy (EDS) was performed on the alternatively sourced nozzle. The EDS spectra revealed a copper-zinc-lead, brass alloy (Figure 26).

Table 1: Chemical Analysis of nozzles C and G (all values are in wt%).

Element	C Used Good	G Bad Lot	Specification
Be	1.94	1.89	1.80 - 2.00
Ni + Co	0.20	0.23	0.20 Minimum
Ni+Fe+Co	0.25	0.27	0.6 Maximum
Ni	0.19	0.23	---
Co	0.01	<0.01	---
Fe	0.05	0.04	---
Al	0.03	0.04	0.20 Maximum
Si	0.04	0.08	0.20 Maximum
Cu	Remainder	Remainder	Remainder
H <sup>1</sup>	<0.001	<0.001	---
Mg	0.06	0.16	---
O <sup>2</sup>	0.002	<0.001	---
Zn	0.01	<0.01	---

---

## Hydrogen-Oxygen Embrittlement of Copper

---

### Review of the Published Literature

A review of the literature on the subject of intergranular cracking of copper alloys revealed that intergranular cracking can occur in copper due to hydrogen embrittlement of oxygen rich copper alloys [1]. Nascent hydrogen penetrates and diffuses through the copper at the grain boundaries during heat treatment in a hydrogen containing atmosphere [2]. The nascent hydrogen then reacts with oxygen present in the copper and form water molecules at the grain boundaries [3]. This causes internal stresses between the material grains, which leads to embrittlement of the material. The grain boundaries of the affected material appear textured (Figure 27) [1]. This is due to micro-void coalescence (i.e. dimpled rupture) around molecules of steam generated in the material [4]. Likewise, intergranular porosity is observed due to water vapor formation at the grain boundaries (Figure 28). This mechanism of failure is described as creep-like, in that it is a delayed failure, occurring after time under load and preferentially at higher temperatures [5].

### Discussion and Conclusion

---

The results of microscopic analysis of the failed nozzles and circumstances of nozzle failure indicate that the most likely cause of nozzle failure was hydrogen-oxygen embrittlement. Recognized mechanisms of intergranular failure in copper are hydrogen-oxygen embrittlement, grain boundary precipitation, and stress corrosion cracking (SCC). Both hydrogen embrittlement and SCC are delayed failure mechanisms, requiring time under load for failure to occur. However, there was no indication that the nozzles were used in a SCC inducing environment (containing ammonia or amines), and lack of branch cracking observed during sample metallography indicates that SCC was not likely the cause of failure. No grain boundary precipitates were observed. The dimpled rupture texturing of the grain boundaries and presence of grain boundary voids observed in nozzles A, B, and G, are consistent with failure from water vapor evolution at the grain boundaries. The location of the failure, separation of the threaded section of the nozzle from the head, was due to the increased stress riser formed by the corner present at the threaded section/head junction. This location is the location of maximum stress, so that the effect of the hydrogen-oxygen embrittlement was exacerbated at this point. Prevention of future failures can be accomplished by selection of low oxygen containing copper alloys, heat-treated in a zero hydrogen environment.

---

## Figures

---



**Figure 1.** Nozzle A in the as-received condition.



**Figure 2.** Nozzle B in the as-received condition.



**Figure 3.** Nozzle C in the as-received condition.



**Figure 4.** Nozzle D in the as-received condition.



**Figure 5.** Nozzles E in the as-received condition.



**Figure 6.** Nozzles F in the as-received condition.





**Figure 7.** Nozzles G in the as-received condition.

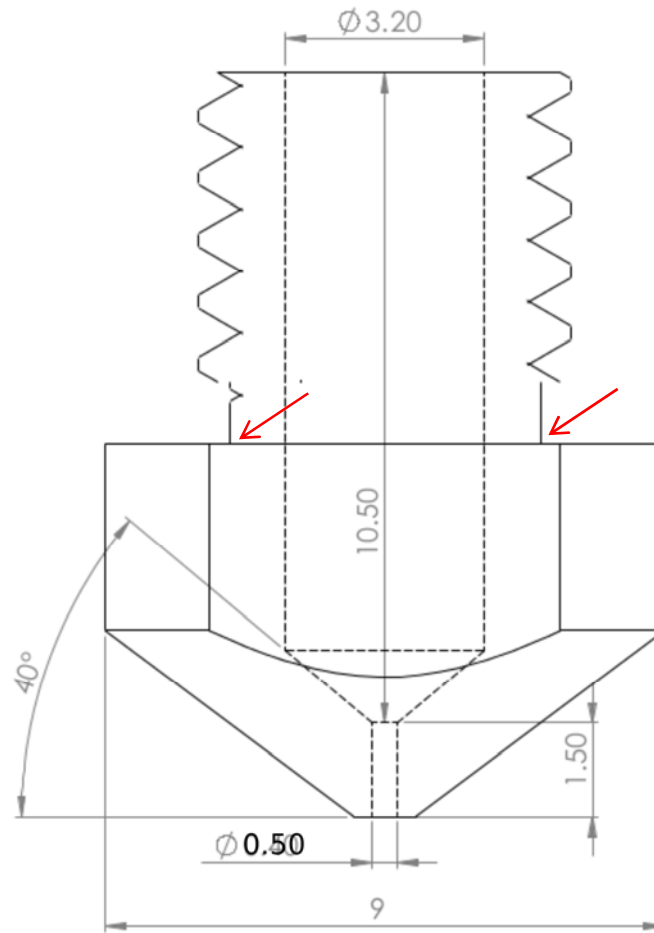


**Figure 8.** Design drawing for the subject nozzle showing the corner at the junction between the threaded section and head and the location of a stress riser (indicated by a red arrows).



**Figure 9.** Stereo-optical microscopy image of the fracture surface of nozzle A showing characteristics (reflectivity) of intergranular fracture.

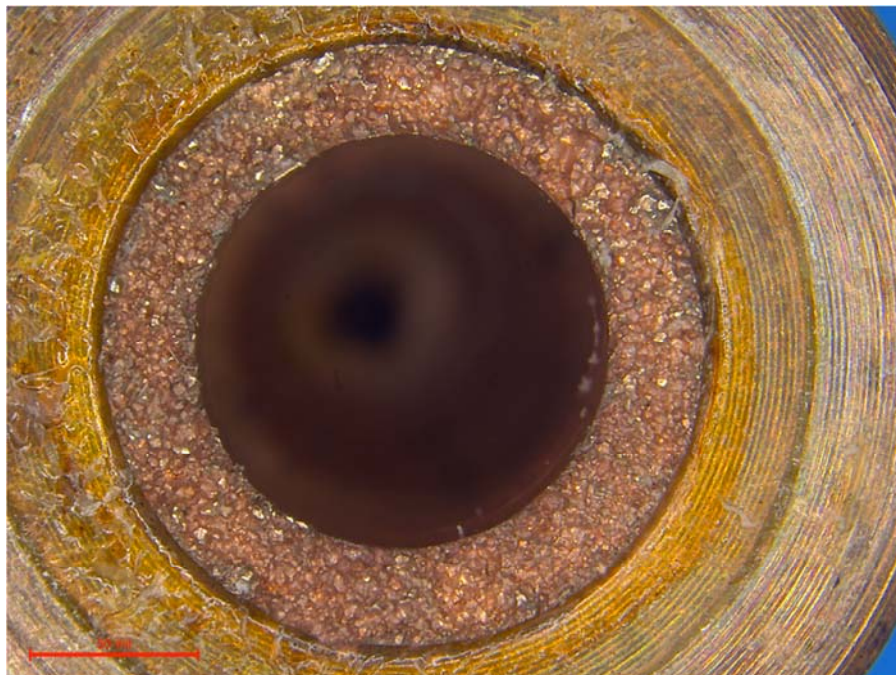


**Figure 10.** Stereo-optical microscopy image of the fracture surface of nozzle B showing characteristics of intergranular fracture.

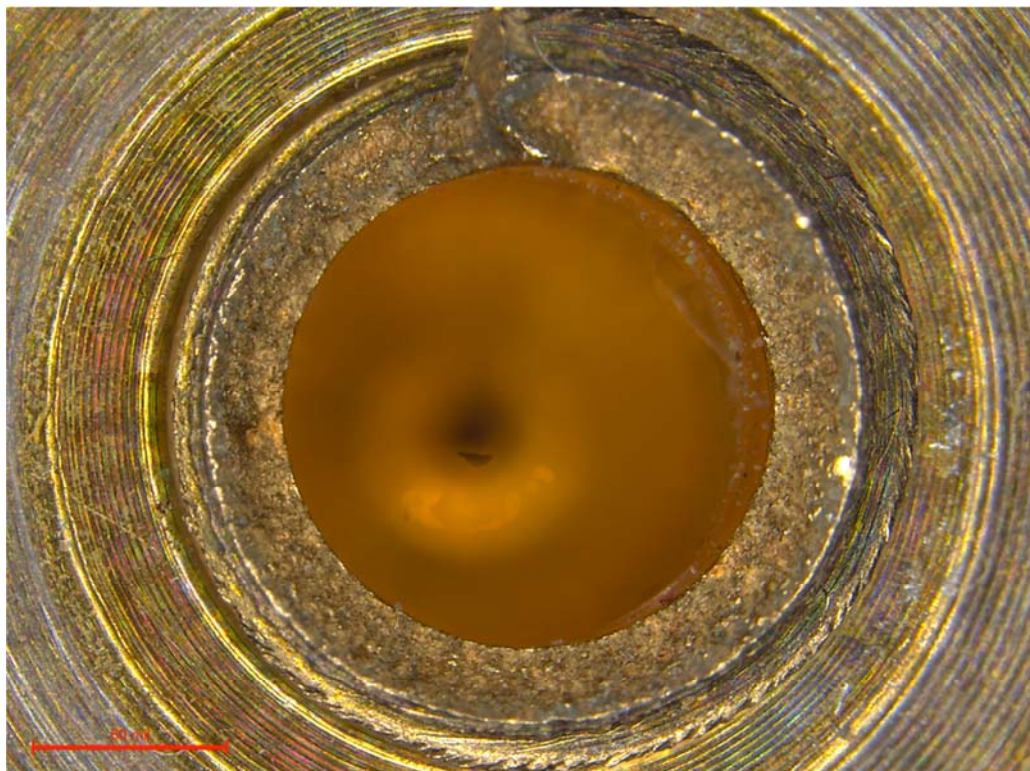


**Figure 11.** Stereo-optical microscopy image of the fracture surface of nozzle F showing characteristics (dull, matte appearance) of ductile overload failure.

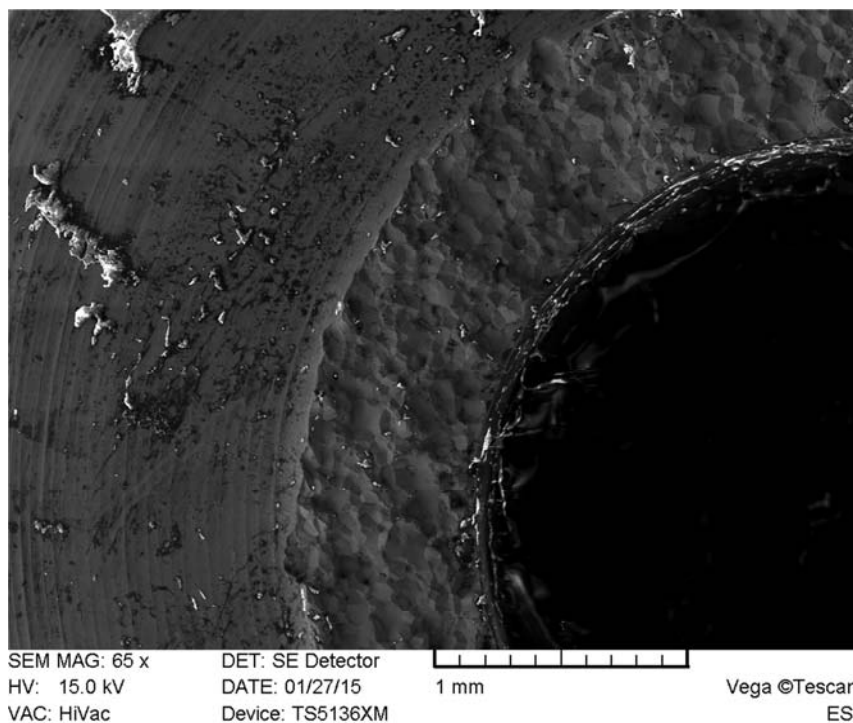


**Figure 12.** SEM image of the fracture surface of nozzle A showing characteristics of intergranular fracture.

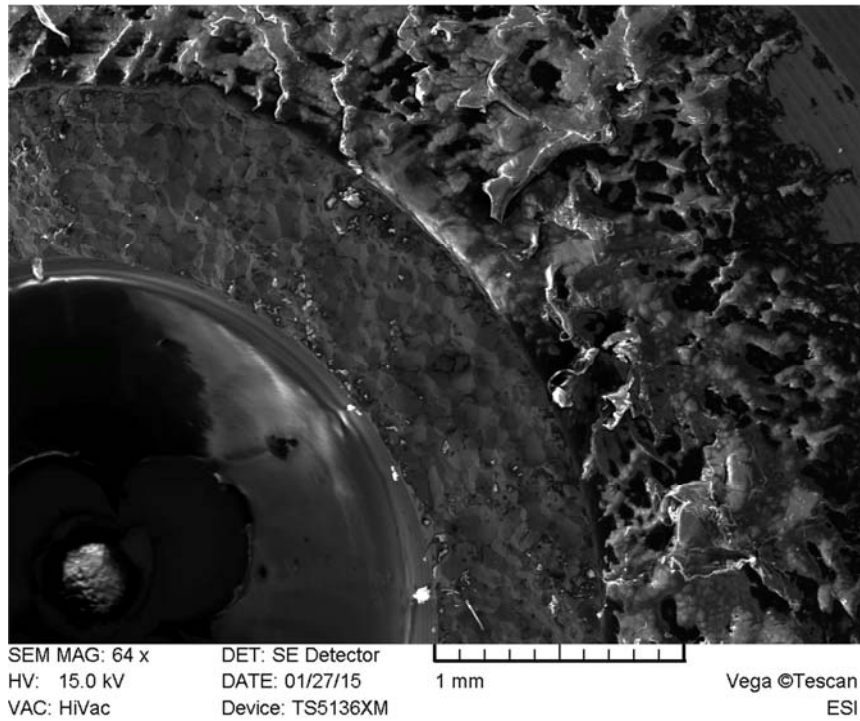
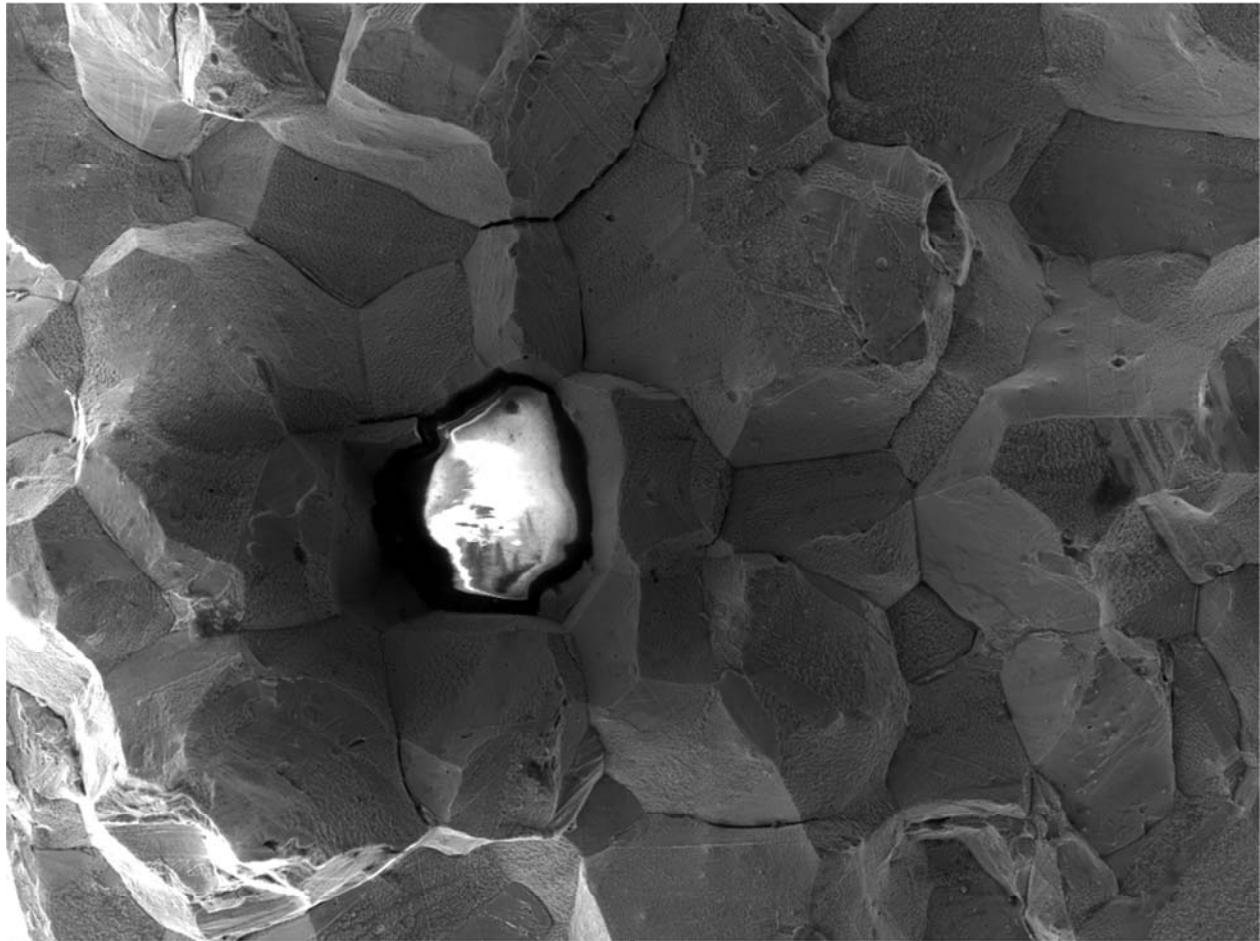


**Figure 13.** SEM image of the fracture surface of nozzle B showing characteristics of intergranular fracture.



SEM MAG: 499 x  
HV: 15.0 kV  
VAC: HiVac

DET: SE Detector  
DATE: 01/27/15  
Device: TS5136XM

200 um

Vega ©Tescan  
ESI

**Figure 14.** SEM image of the fracture surface of nozzle B showing intergranular fracture and dimpled rupture of the grain boundary surfaces. Note the presence of adhered polymeric residue (the white “charging” particle) to the fracture surface.

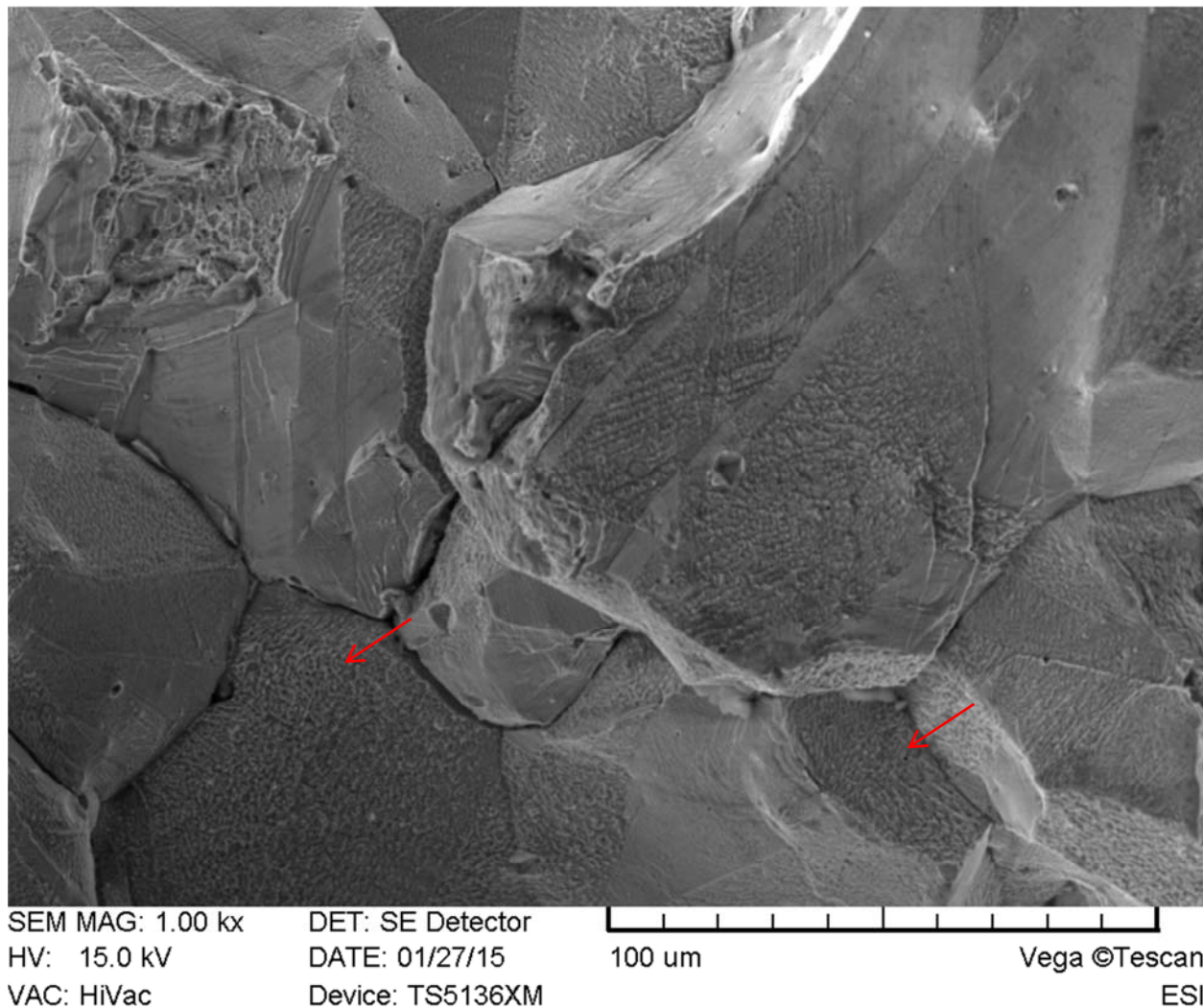


**Figure 15.** SEM image of the fracture surface of nozzle B showing intergranular fracture and dimpled rupture of the grain boundary surfaces (identified with red arrows).

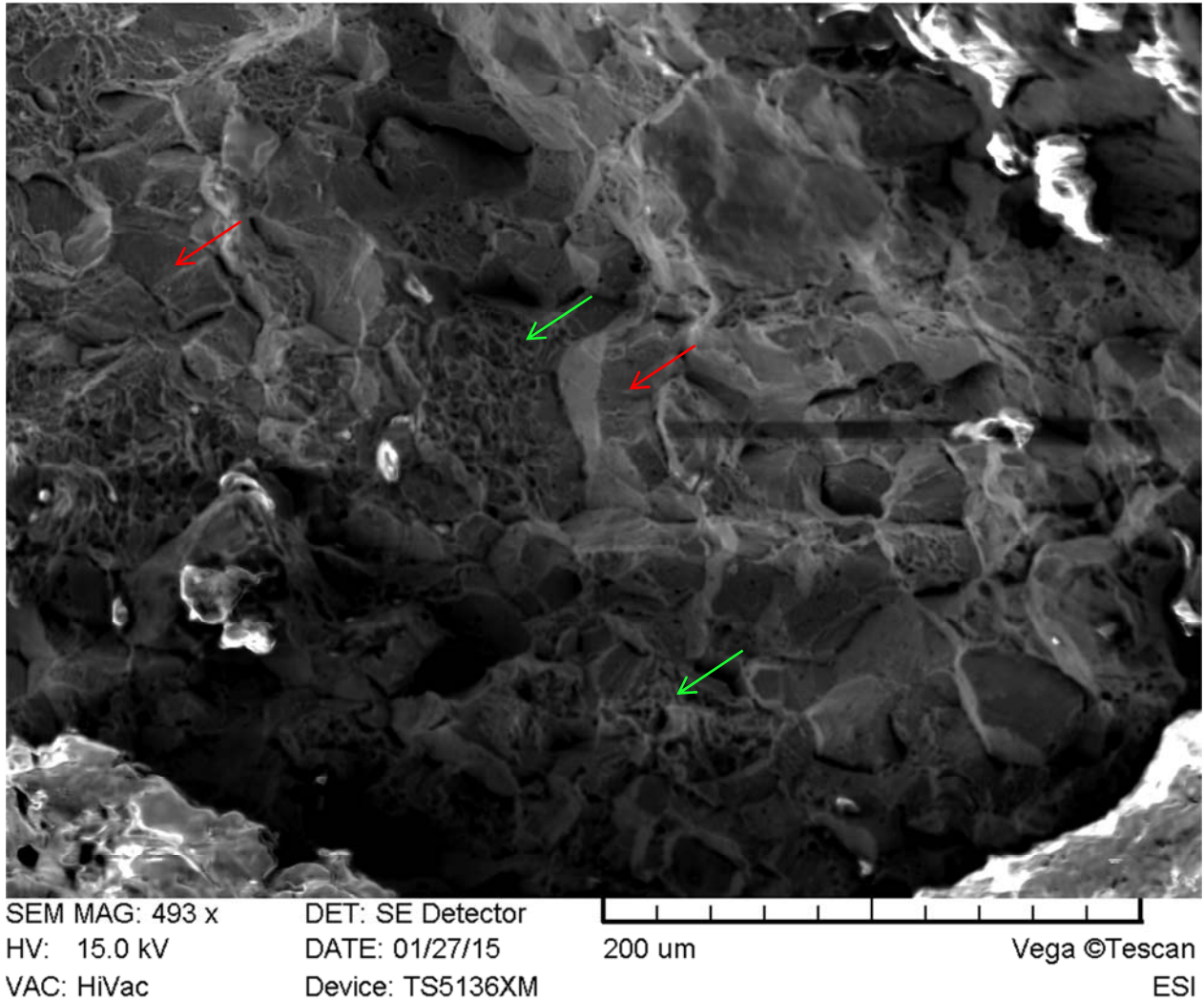


**Figure 16.** SEM image of the fracture surface of nozzle F showing mixed mode intergranular fracture (identified with red arrows) and dimpled rupture of ductile overload (identified with green arrows).



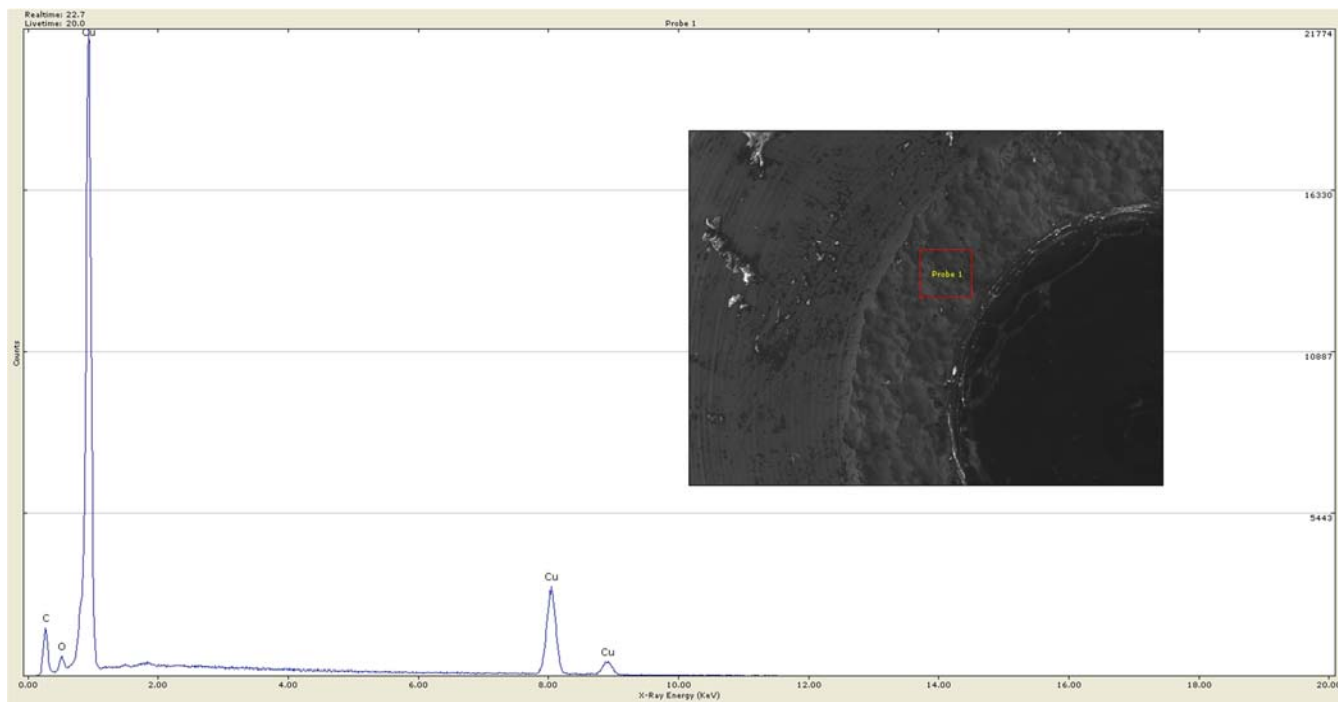


**Figure 17.** EDS spectra and locator map for the analysis of nozzle A showing the presence of copper, oxygen, and carbon.

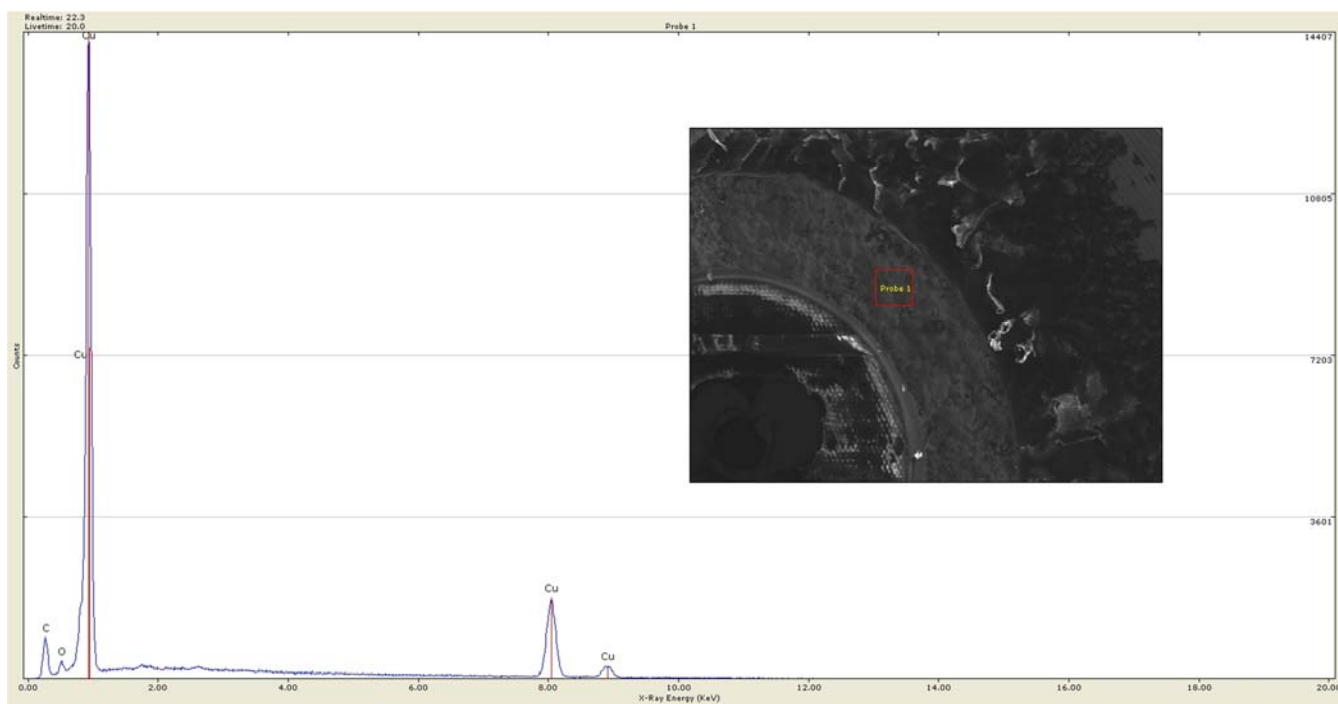


**Figure 18.** EDS spectra and locator map for the analysis of nozzle B showing the presence of copper, oxygen, and carbon.

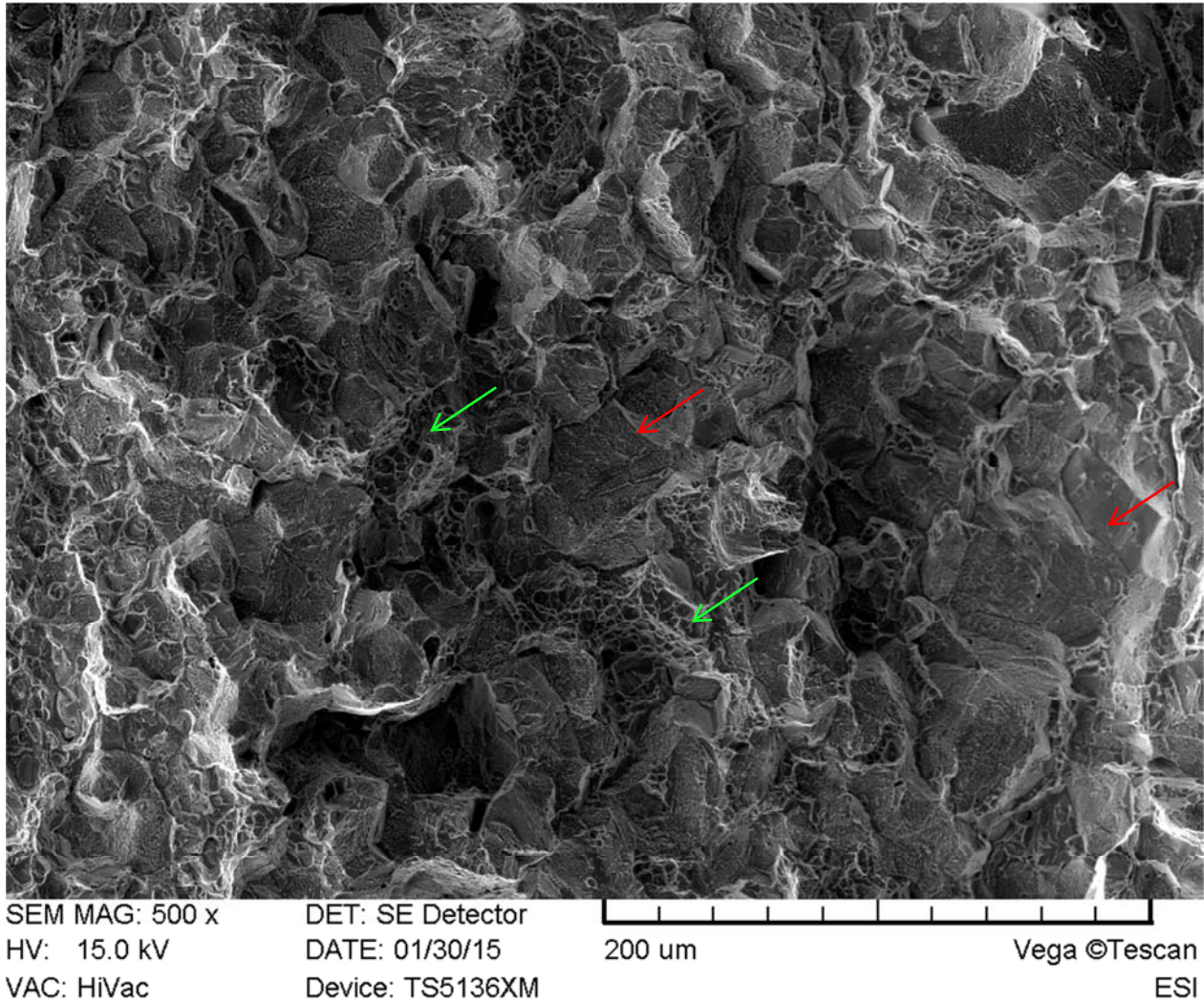
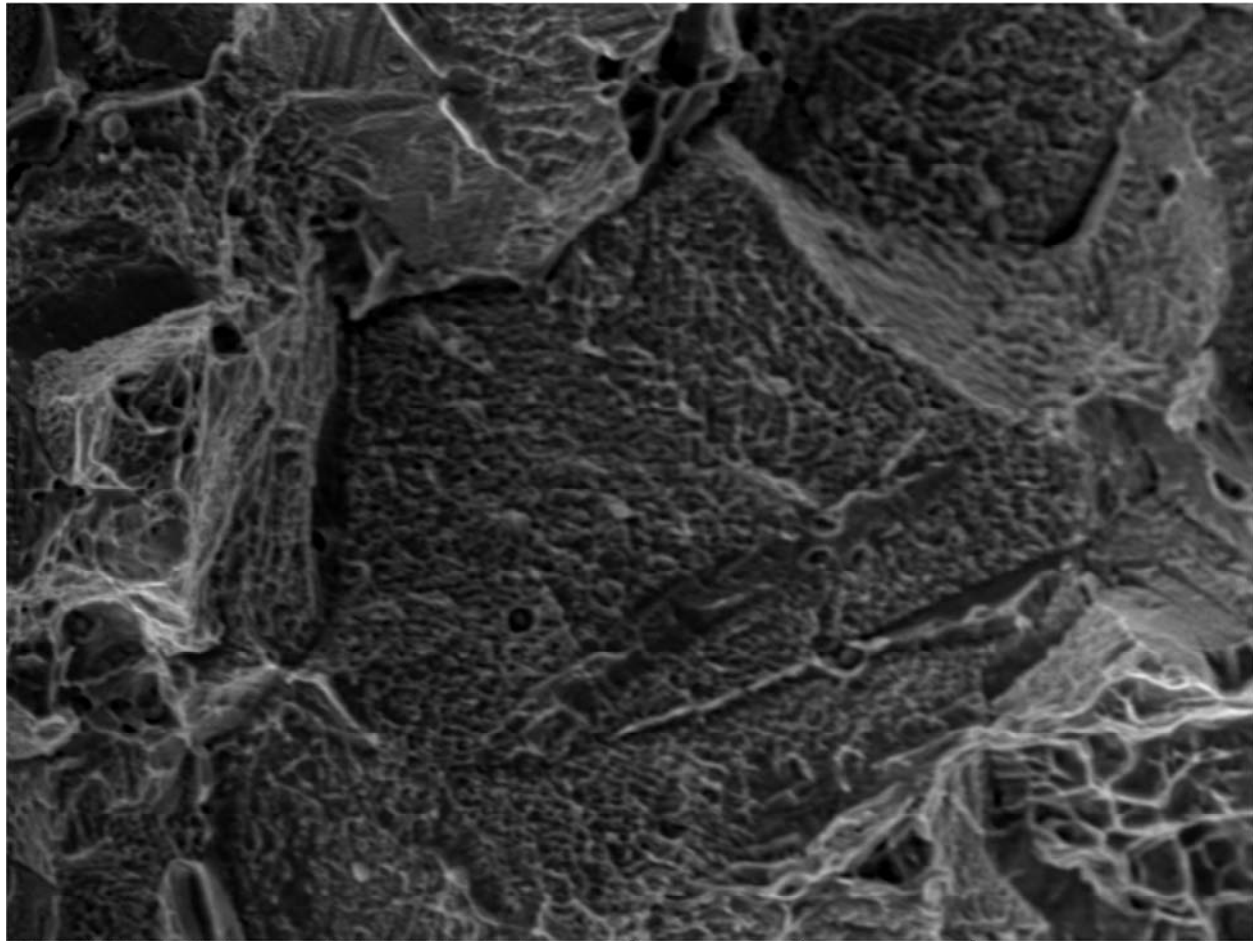


**Figure 19.** SEM image of the fracture surface of the threaded section of nozzle G showing mixed mode intergranular fracture (identified with red arrows) and dimpled rupture of ductile overload (identified with green arrows).



SEM MAG: 2.99 kx      DET: SE Detector      20 um  
HV: 15.0 kV      DATE: 01/30/15  
VAC: HiVac      Device: TS5136XM      Vega ©Tescan  
ESI

**Figure 20.** SEM image of the fracture surface of the threaded section of nozzle G showing dimpled rupture at the grain boundaries of the material.

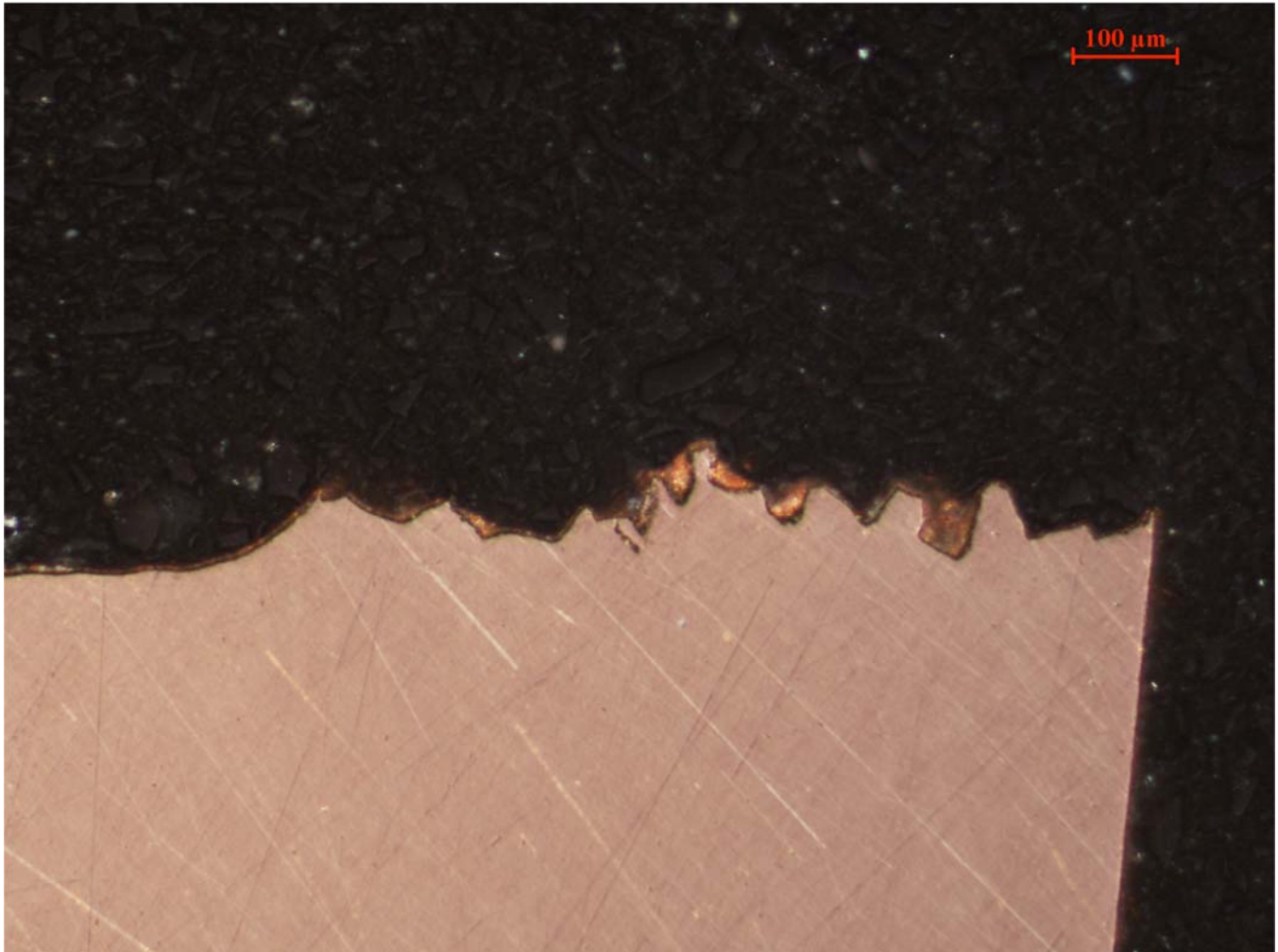


**Figure 21.** Metallography of the cross section of the head of nozzle A at the fracture surface showing a lack of branch cracking, which would be indicative of SCC.

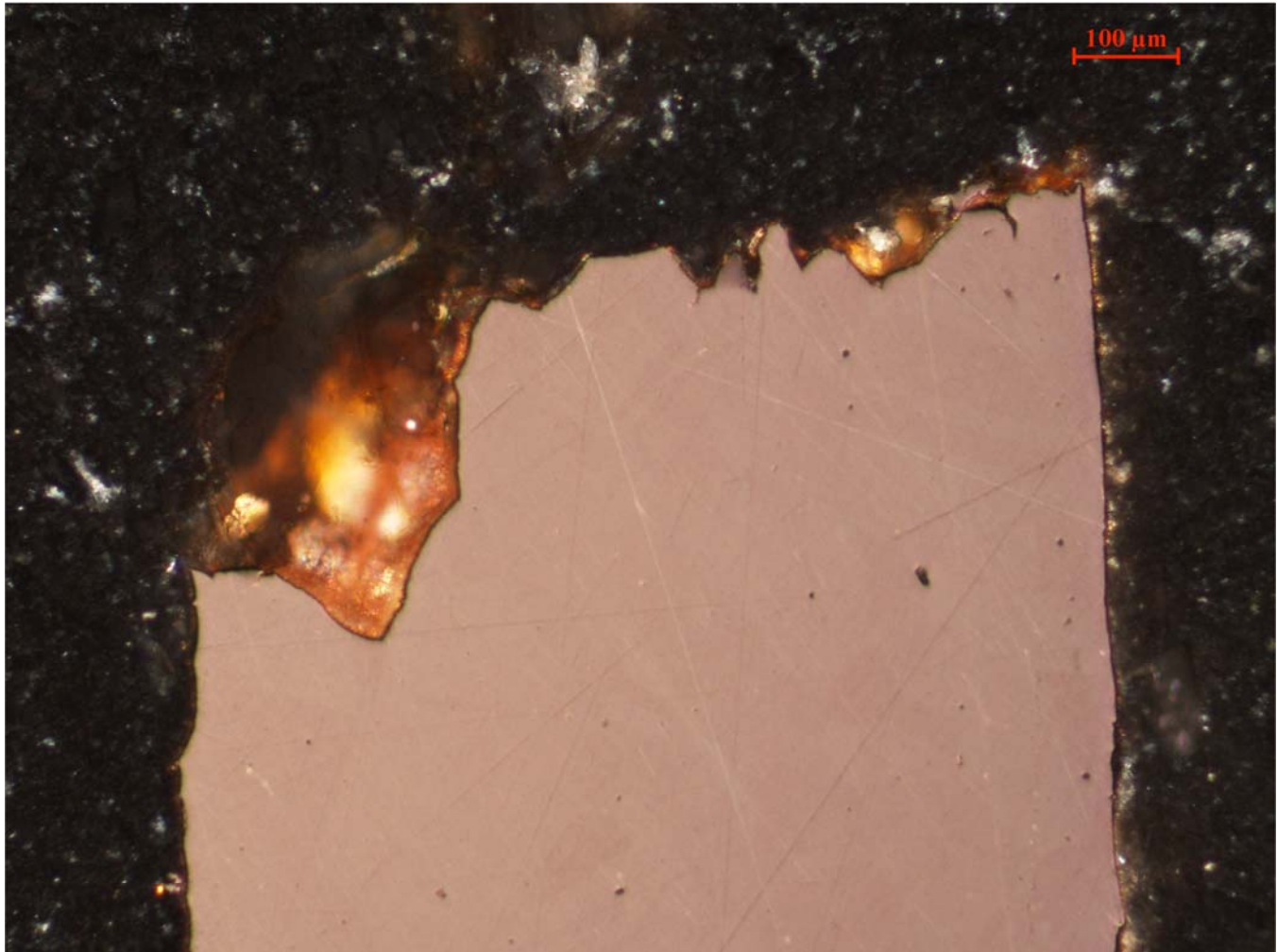


**Figure 22.** Metallography of the cross section of the threaded section of nozzle A at the fracture surface showing a lack of branch cracking.

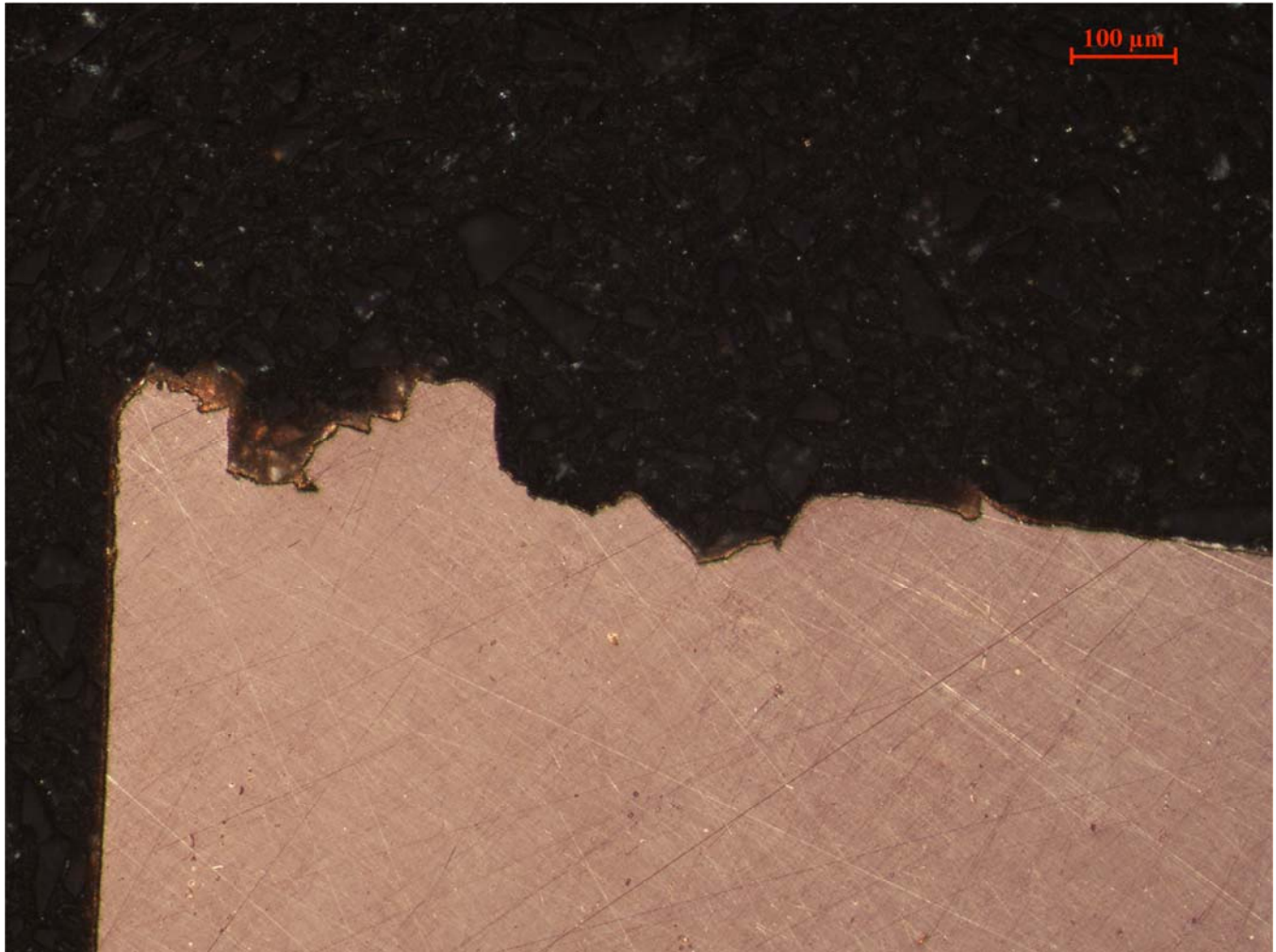
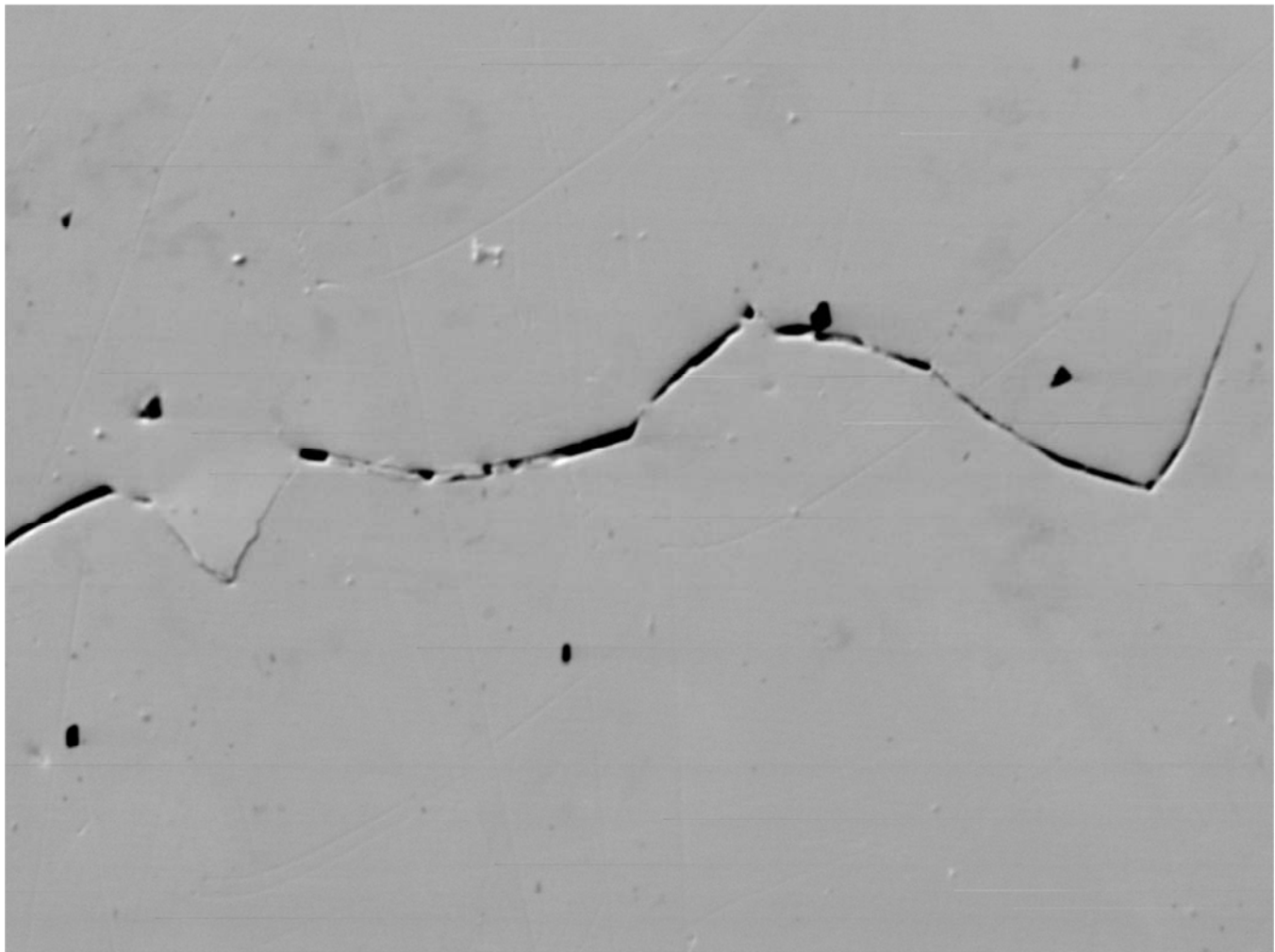


**Figure 23.** Metallography of the cross section of the head of nozzle B at the fracture surface showing a lack of branch cracking.



**Figure 24.** Metallography of the cross section of the threaded section of nozzle A showing grain boundary cracking as a series of interconnected voids.



SEM MAG: 750 x  
DET: SE Detector  
HV: 15.0 kV

Name: 47357A\_A\_05  
DATE: 02/03/15

100 um

Vega ©Tescan  
ESI  
47357A

**Figure 25.** SEM image of the cross section of the threaded section of nozzle A showing grain boundary cracking as a series of interconnected voids.



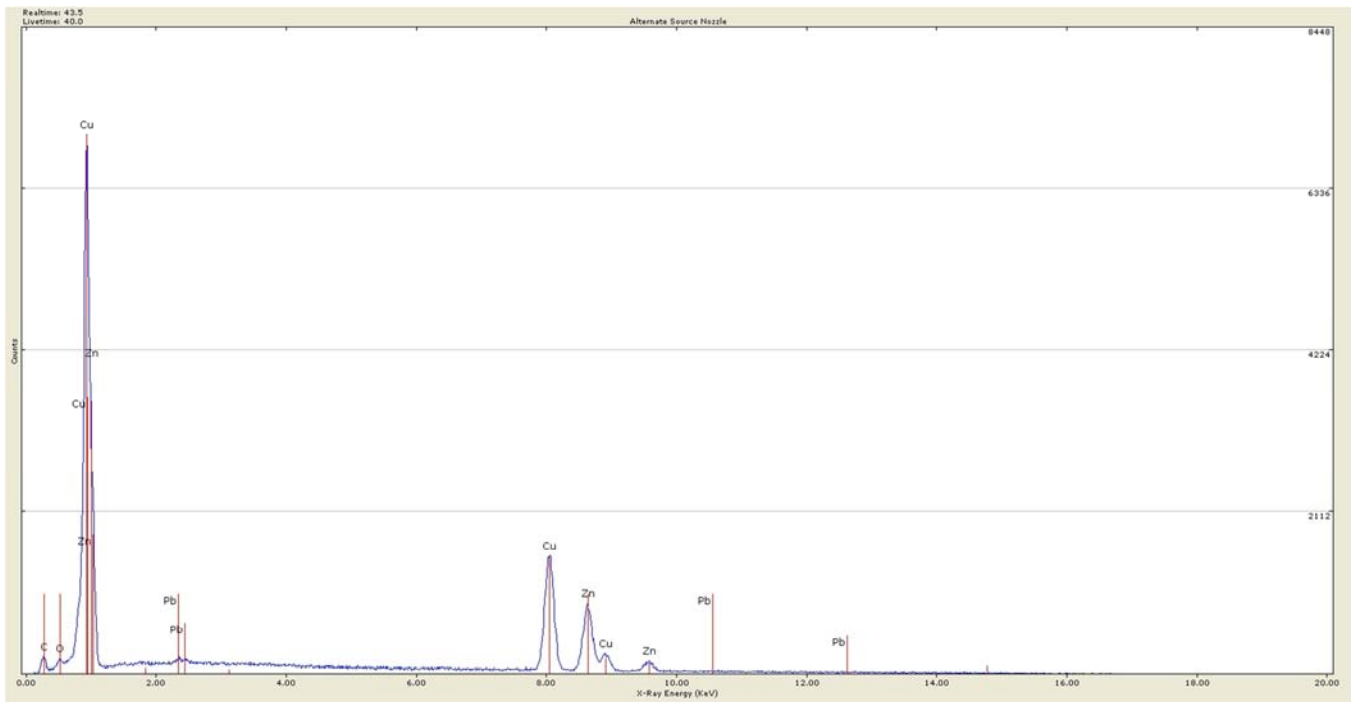


**Figure 26.** EDS spectra for the analysis of the alternatively sourced nozzle showing the presence of copper, zinc, lead, oxygen, and carbon, indicative of a brass alloy.

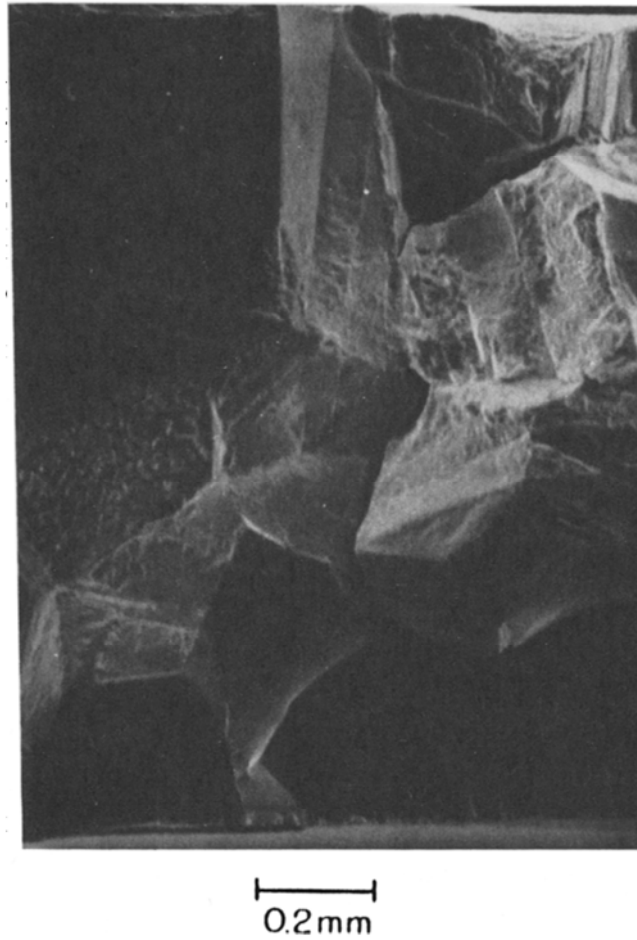


**Figure 27.** Texturing on the grain boundaries in intergranular fracture of oxygen-saturated copper from hydrogen embrittlement [1].

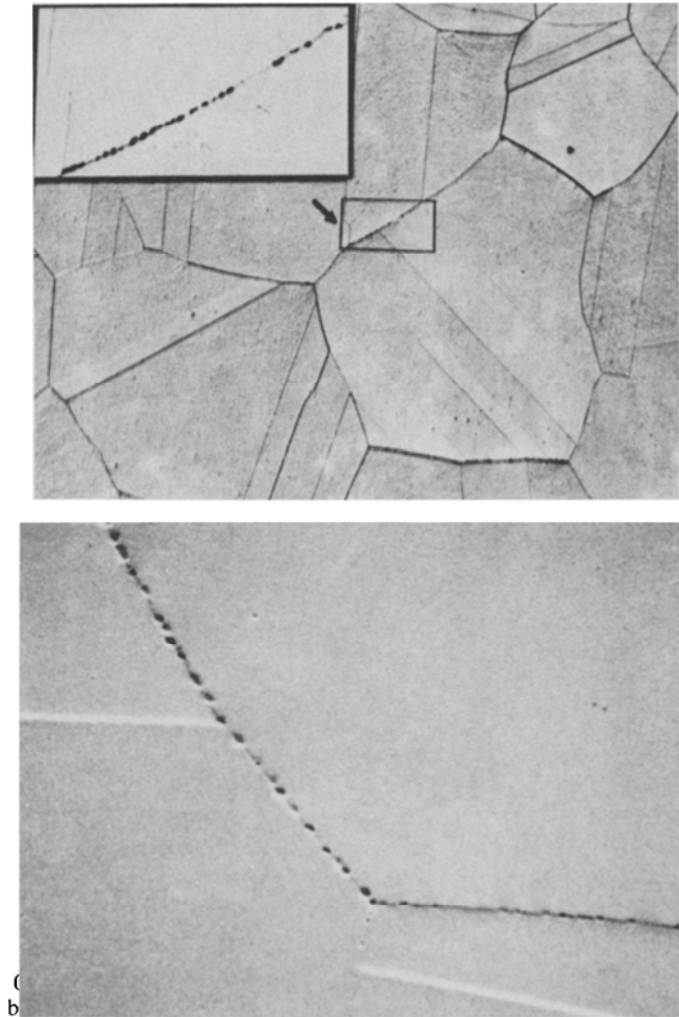


**Figure 28.** Metallographic images of voids or bubbles formed at the grain boundaries due to water vapor evolution in oxygen-saturated copper from hydrogen embrittlement [1].

---

## References

---

1. Neih, T.G., Nix, W.D. Embrittlement of Copper Due to Segregation of Oxygen to Grain Boundaries. Metallurgical Transactions A, Volume 12A, May 1981, 893-901
2. Matting, A., Ziegler, Ruth. Brittleness in Copper and Copper Alloys With Particular Reference to Hydrogen Embrittlement. Hydrogen Damage and Embrittlement, Failure Analysis and Prevention, Vol 11, ASM Handbook, ASM International, 2002, p 809–822
3. Woodford, D.A., Bricknell, R.H. Environmental Embrittlement of High Temperature Alloys by Oxygen. Treatise on Materials Science and Technology, Volume 25. London, UK: Academic Press, Inc., 1983.
4. Louthan, M.R. Hydrogen Embrittlement of Metals: A Primer for the Failure Analyst. U.S. Department of Energy. WSRC-STI-2008-00062
5. Walker, Gavin. Solid State Hydrogen Storage: Materials and Chemistry. Boca Raton, FL: CRC Press, 2008.
6. Mattsson, E., Shuckher, F. An Investigation of Hydrogen Embrittlement in Copper. Journal of the Institute of Metals, Volume 87, 1959